# Supplementary Methods

### Anthropometric and biochemical measurements

Blood pressure was measured using a Marquette Dash 300 monitor (GE Healthcare, Little Chalfont, Bucks, UK) as previously described [1]. Fasting glucose, insulin, haemoglobin A1c (HbA1c), total cholesterol, high-density lipoprotein (HDL)-cholesterol, triglyceride, non-esterified fatty acid (NEFA), alanine aminotransferase (ALT), aspartate aminotransferase (AST), adiponectin, leptin, high-sensitivity C-reactive protein (hs-CRP), tumour necrosis factor-α (TNFα), interleukin (IL)-6, IL-8 and IL-10, hyaluronic acid (HA), propeptide of type 3 procollagen (P3NP), tissue inhibitor of metallo-proteinases-1 (TIMP-1), growth differentiation factor 15 (GDF-15), follicle-stimulating hormone (FSH), and oestradiol concentrations were measured in serum samples using commercially available kits according to the manufacturer's instructions. Concentrations of GDF-15, leptin and adiponectin were measured in fasting serum samples by the Cambridge Biochemical Assay Laboratory, University of Cambridge. Presence of the metabolic syndrome (MetS) was diagnosed as previously described [2].

### Adipocyte cell size quantification and SAT collagen staining

Adipocyte cell size was quantified using H&E-stained formalin-fixed paraffin-embedded human SAT sections (5 μm) and via Picrosirius red staining were performed as previously reported [3]. Histology images were captured using an Olympus VS120 slide-scanning system with an integrated Allied Vision Technologies Pike camera (Olympus Corporation, Shinjuku, Tokyo, Japan) at 10x magnification using an Olympus UPlanSApo 10x objective with 0.75 NA at room temperature within the Biomedical Imaging Unit (University of Southampton, Southampton General Hospital). Acquisition software used was Olympus VS-ASW-L100 version 2.9 (Olympus Corporation, Shinjuku, Tokyo, Japan).

**Multiphoton second-harmonic generation and two-photon fluorescence microscopy and image processing**

Unstained formalin-fixed paraffin-embedded human SAT sections (5 µm) from patient biopsies that gave the lowest and highest CCGE z-scores (n = 3 per group) were imaged using a custom-built multiphoton laser scanning microscope at the University of Southampton. Unstained sections and sections used for Picrosirius red staining were taken in series. The output at 797.5 nm from a *pico*Emerald™ S (APE, 2 ps, 80 MHz) was directed into a Zeiss LSM confocal microscope with an Axio Examiner upright microscope (LSM 980). The internal optics was used to direct the beam into a 10x 0.5 NA objective (421440-9900-000, Zeiss) that was used for all experiments. The laser power on the sample was 70mW. The resultant SHG signal was detected in a back reflected (epi) configuration with non-descanned detection using a multi-alkali photomultiplier tube (PMT), Hamamatsu r6357. A band pass filter 400+/-20 nm (FBH400-40, Thorlabs) was used to isolate the SHG signal. The voltage gain for all SHG images was set to 800V for all images. Two photon excited autofluorecence (TPF) was detected in a transmission, using a condenser (1.2NA) before being detected by a gallium arsenide phosphide (GaAsP) detector set to 600V. Here a 525-25 nm band pass filter was used. All SHG and TPF images were taken at 4363 pixels by 4363 pixels with pixel dwell time of 0.48 µs and each frame was an average of 2 repeats. The z-stack were either 11 or 13 frames with steps of 2 µm between each slice. Brightfield images were taken with a Zeiss Axiocam 305 using the Halogen lamp. Kohler illumination was used, and images were captured with an exposure time of 1 ms with an intensity of 2 V. Image processing was performed with FIJI v2.14.0. For each Z-stack and channel, a single sum intensity image was generated from 11-13 images followed by pseudo colour assignment to each channel (Cyan for SGH and red for TPF). The background was reduced by a blur function which replaced each pixel with the average of the 3x3 neighbours and by a rolling ball background subtraction (50 pixels). Consistent and uniform adjustment for brightness and contrast was carried out on all images. Individual and composite image files (.tiff format) were then used to compile figures in Adobe Illustrator v2023.

**Abdominal magnetic resonance imaging**

MRI of patients was carried out by Dr Angela Darekar (UHS, NHS England). The MRI technique utilises the body's natural magnetic properties to produce detailed images of the body using the hydrogen nucleus (i.e. a single proton) due to its abundance in water and fat. Images were acquired from five non-contiguous slices of the abdomen, extending from 5 cm below to 15 cm above L4–L5, to obtain a more accurate estimation of visceral fat than from a single slice. Axial scans were acquired with participants in the supine position. Participants were scanned on a 1.5T MR scanner (Siemens Avanto, Syngo software release B17; Siemens AG, Munich, Germany) using a 32-channel body coil. A gradient echo 2D FLASH (fast low-angle shot) sequence (TR = 111 ms, TE = 4.18 ms, flip angle = 70°, slice width = 10 mm, slice spacing = 50 mm) was used to obtain T1-weighted images. T1 (longitudinal relaxation time) is the time constant which determines the rate at which excited protons return to equilibrium (i.e. time taken for spinning protons to realign with the external magnetic field). In order to accommodate the circumference of the individual being scanned within the image, the field of view was varied. The MR images were analysed using a proprietary software package (Mimics 14.0; Materialise NV, Leuven, Belgium) to identify regions of subcutaneous and visceral fat within the cross-sectional abdominal MR images. This package enabled the use of thresholding methods to identify regions of subcutaneous and visceral fat. By examining the histogram of pixel values present in the image, threshold levels could be set, and as fat pixels were the highest value pixels in the image, fat tissue could be segmented out from other tissue in the images. Some manual intervention was required when using this technique, as there was some variation in signal intensity across the image, which is often the case in large field-of-view MR images. Three different masks were created: one comprising the whole cross-section of the body, one containing the visceral fat region and one containing the subcutaneous fat region. It was possible to determine the number of pixels contained within each of these masks, and hence calculate the areas (and volumes) of subcutaneous fat and

visceral fat and compare them with the total cross-sectional area. Adipose tissue volume was converted to mass in kg using a density of 0.92 kg/l for adipose tissue.

**RNAseq data processing and DGE analysis**

Raw data from RNA sequencing were provided in the format of FASTQ files. FASTQ sequence quality was assessed using FASTQC software[4] and results merged with the MultiQC [5] tool. Raw paired end sequencing reads were then aligned to the GRCh38 human reference genome using STAR (v2.7.9a) with ENCODE options and two pass mode. The resulting BAM files were sorted and indexed using Samtools (v1.9) [6]. After alignment, the quality of the aligned files was assessed using RSeQC [7] and all sequenced samples passed the quality control assessment. All referenced files were downloaded from the GENCODE [8] online repository release 38.

The number of raw read counts was determined with HTseq (v0.6.1) [9] using union mode. The bioinformatic analysis of the RNA sequencing data were analysed using EdgeR packages by Dr Carolina Oquendo. Only protein coding autosomal genes were included in the RNAseq analysis. To test for differential gene expression (DGE) in RNAseq data, the quasi-likelihood pipeline of edgeR was used. This pipeline fits the data to a genewise negative binomial generalized linear model, using the generalized linear model (GLM) functionality. DGE analysis was performed on protein coding autosomal genes only and *P*-values were adjusted using the Benjamini-Hochberg method. Paired DGE analysis exploring the potential impact of synbiotic treatment was done according to the use of a custom design matrix that is described elsewhere[10]. Venn diagrams were constructed using InteractiVenn (http://www.interactivenn.net) [11]. Heatmaps were made with the ComplexHeatmap package in R using a matrix of scaled log counts per million after TMM normalisation (EdgeR). Columns were grouped by fibrosis status and hierarchical clustering was carried out using the default Euclidean distance. To investigate the enrichment of functional biological processes in the differentially expressed gene lists, Gene set enrichment analysis (GSEA) analysis against MSigDB Hallmark [12], Reactome [13] and Kyoto Encyclopedia of Genes and Genomes (KEGG) [14] gene sets was performed using clusterProfiler [15] in R. The gene symbols from the list were converted to entrez IDs

using the org.Hs.eg.db library and used as input. The log fold changes for the genes tested in the DGE analyses were extracted and used as input into the GSEA() function in R package clusterProfiler with gene sets obtained using the msigdbr() functions of the msigdbr R package. The GSEA() function was run using default parameters.

**Supplementary table 1 – AdipoIR is associated with the presence of ≥F2 liver fibrosis at baseline.**

| Variables | OR (95% CI) | *P* value |
|---|---|---|
| Sex (M vs. F) | 1.37 (0.34-5.49) | 0.66 |
| Age (years) | 0.96 (0.91-1.02) | 0.23 |
| T2DM status (yes) | 1.97 (0.39-10.02) | 0.42 |
| AdipoIR | 1.03 (1.01-1.06) | **0.02** |
| GDF-15 (pg/ml) | 1.002 (1.000-1.003) | 0.07 |

Dependent variable was liver VCTE measurements <8.2 vs. ≥8.2 kPa (0 and 1, respectively) as a proxy threshold for the non-invasive identification of ≥F2 fibrosis. This regression model was statistically significant (X2(5) = 21.4, P=0.001. Hosmer and Lemeshow Test P=0.50. Collectively, the explanatory variables in this regression model explained 42.2% of the variance in the dependent variable. Covariates considered were age and sex to account for any potential influence/interaction with AdipoIR, T2DM given the increased prevalence in patients with ≥F2 fibrosis and GDF-15 concentrations as we have previously found this protein to be strongly associated with liver fibrosis severity in patients with NAFD Sample size n=58. Note: addition of BMI, total body adiposity or leptin concentrations to this model did not affect the statistical significance of the model (data not shown).

**Supplementary Table 2 -** Baseline and end-of-study results of inflammatory markers and adipokines and regression models testing the effect of the synbiotic treatment on inflammatory markers and adipokines.

| | **Placebo (n=33)** | | **Synbiotic (n=29)** | | **Difference in change from baseline to end of study* (95% CI) Synbiotic treatment Primary analysis** | **Adjusted difference in change from baseline to end of study** (95% CI) Synbiotic treatment Primary analysis** |
|---|---|---|---|---|---|---|
| | **Baseline** | **End of study** | **Baseline** | **End of study** | | |
| IL-6 (pg/ml) [a] | 3.1 (1.6) | 1.5 (1.7) | 2.6 (1.4) | 1.3 (1.0) | 0.07 (0.05-0.19) P = 0.28 | 0.07 (-0.04-0.19) P = 0.21 |
| IL-8 (pg/ml) [a] | 15.7 (11.2) | 14.2 (7.6) | 14.0 (10.8) | 15.6 (8.8) | -0.02 (-0.10-0.06) P = 0.63 | -0.01 (0.09-0.07) P = 0.84 |
| IL-10 (pg/ml) [a] | 0.8 (0.5) | 0.6 (0.2) | 0.8 (0.4) | 0.6 (0.3) | 0.003 (-0.09-0.01) P = 0.96 | -0.02 (-0.11-0.08) P = 0.74 |
| TNFα (pg/ml) [a] | 10.3 (5.8) | 10.1 (5.1) | 13.0 (5.6) | 11.1 (5.4) | -0.11 (-0.35-0.13) P = 0.36 | -0.07 (-0.31-0.16) P = 0.54 |
| MCP-1 (pg/ml) [a] | 271.7 (144.4) | 224.0 (100.5) | 291.3 (151.4) | 215.5 (132.9) | 14.4 (-15.3-44.2) P = 0.33 | 14.4 (-16.5-45.3) P = 0.36 |
| hsCRP (mg/L) | 3.0 (3.5) | 3.0 (5.5) | 4.0 (4.5) | 2.0 (4.0) | 0.11 (-0.04-0.25) P = 0.14 | 0.07 (-0.07-0.21) P = 0.33 |
| GDF-15 (pg/ml) | 906.1 (782.8) | 865.4 (883.7) | 885.5 (684.4) | 1059.1 (779.5) | -0.02 (-0.07-0.03) P = 0.38 | -0.03 (-0.8-0.2) P = 0.19 |
| Leptin (ng/ml) | 27.8 (30.3) | 26.3 (25.3) | 21.0 (33.2) | 18.5 (29.5) | 0.06 (-0.01-0.14) P = 0.09 | 0.04 (-0.02-0.10) P = 0.23 [b] |
| Adiponectin (µg/ml) | 3.9 (2.8) | 4.5 (2.8) | 4.7 (4.2) | 4.4 (4.4) | -0.01 (-0.05-0.03) P = 0.70 | -0.004 (-0.05-0.04) P = 0.86 |

| | | | | | | |
|---|---|---|---|---|---|---|
| SAT CCGE values | 0.2 (0.1) | 0.3 (1.0) | -0.2 (0.7) | 0.01 (0.80) | -0.06 (-0.40-0.28) P = 0.71 | -0.9 (-0.4-0.26) P = 0.62 |

Results of multivariable linear regression models testing the effects of synbiotic treatment on changes in inflammatory markers, adipokines and SAT CCGE values between baseline and end of study. Baseline and end of study data are shown as median (IQR). For each pre-specified outcome the difference in outcome represents the change in the outcome between baseline and end of study. In order to generate normally distributed differences in outcome measurements, delta measurements were generated from logarithmically transformed baseline and end of study measurement note – a square root transformation was used for TNFα concentrations. Differences in the transformed end of study and baseline measurements (i.e. delta values) were entered as outcome variables.* adjusted for baseline measurement of the outcome variable only, or ** adjusted for baseline measurement of the outcome plus age, sex, weight difference and baseline weight. n= 33 vs 29, [a]n=33 vs 28 [b]. Analysis was not adjusted for sex as in introduced issues of collinearity.

**Supplementary table 3 -** Baseline and end-of-study results of inflammatory markers and adipokines and regression models testing the effect of the synbiotic treatment on inflammatory markers and adipokines in whole INSYTE cohort.

| | **Placebo (n=44)** | | **Synbiotic (n=44)** | | **Difference in change from baseline to end of study* (95% CI) Synbiotic treatment Primary analysis** | **Adjusted difference in change from baseline to end of study** (95% CI) Synbiotic treatment Primary analysis** |
|---|---|---|---|---|---|---|
| | **Baseline** | **End of study** | **Baseline** | **End of study** | | |
| IL-6 (pg/ml) | 2.9 (1.7) | 1.5 (1.4) | 2.4 (1.6) | 1.3 (0.9) | 0.08 (-0.05 – 0.21) P = 0.25 | 0.08 (-0.05 – 0.21) P = 0.24 |
| IL-8 (pg/ml) | 15.6 (10.5) | 13.3 (5.1) | 14.2 (9.5) | 15.2 (8.1) | -0.06 (-0.12 – 0.01) P = 0.09 | -0.06 (-0.12 – 0.01) P=0.08 |
| IL-10 (pg/ml) | 0.8 (0.5) | 0.6 (0.2) | 0.7 (0.4) | 0.6 (0.3) | -0.05 (-0.15 – 0.04) P = 0.27 | -0.06 (-0.15 – 0.03) P = 0.19 |
| TNFα (pg/ml) | 10.7 (5.7) | 10.1 (5.2) | 12.3 (5.3) | 12.2 (5.9) | -0.05 (-0.10 – 0.01) P = 0.09 | -0.04 (-0.10 – 0.01) P = 0.13 |
| MCP-1 (pg/ml) | 269.0 (143.0) | 210.0 (98.0) | 269.0 (143.0) | 204.0 (117.5) | -0.01 (-0.06 – 0.04) P = 0.71 | -0.01 (-0.06 – 0.05) P = 0.77 |
| hsCRP (mg/L) | 2.7 (3.8) | 3.0 (5.5) | 2.0 (4.0) | 2.0 (4.0) | 0.10 (-0.03 – 0.22) P = 0.12 | 0.07 (-0.05 – 0.18) P = 0.27 |
| GDF-15 (pg/ml) | 762.2 (752.0) | 808.5 (733.0) | 764.0 (708.4) | 895.0 (778.0) | -0.03 (-0.07 – 0.01) P = 0.17 | -0.03 (-0.07 – 0.003) P = 0.07 |
| Leptin (ng/ml) | 26.2 (30.4) | 25.4 (27.7) | 21.0 (37.9) | 18.5 (30.9) | 0.05 (-0.01 – 0.11) P = 0.11 | 0.02 (-0.02 – 0.07) P = 0.32 |
| Adiponectin (µg/ml) | 4.4 (2.6) | 4.9 (2.6) | 4.3 (2.6) | 4.4 (3.3) | -0.01 (-0.05 – 0.02) P = 0.52 | -0.01 (-0.04 – 0.03) P= 0.69 |

Results of multivariable linear regression models testing the effects of synbiotic treatment on changes in inflammatory markers, adipokines and SAT CCGE values between baseline and end of

study. Baseline and end of study data are shown as median (IQR). For each pre-specified outcome, the difference in outcome represents the change in the outcome between baseline and end of study. To generate normally distributed differences in outcome measurements, delta measurements were generated from logarithmically transformed baseline and end of study measurement note – a square root transformation was used for TNFα concentrations. Differences in the transformed end of study and baseline measurements (i.e. delta values) were entered as outcome variables. * Adjusted for baseline measurement of the outcome variable only, or ** adjusted for baseline measurement of the outcome plus age, sex, weight difference and baseline weight.

**Supplementary Table 4** - Results of GSEA between patients with vs without ≥F2 fibrosis suggest that annotations linked with inflammation and tissue remodelling are enriched in SAT with increased liver fibrosis severity.

| | NES | Adjusted *P* value |
|---|---|---|
| Hallmark Gene Set (50 gene sets) | | |
| **Epithelial Mesenchymal Transition** | 2.29 | 1.3E-09 |
| **Inflammatory Response** | 2.16 | 1.3E-09 |
| **TNFα Signalling via NFκB** | 2.10 | 1.3E-09 |
| **IL6 JAK Stat3 Signalling** | 2.10 | 3.6E-07 |
| **E2F Targets** | 1.92 | 3.4E-07 |
| **G2M Checkpoint** | 1.91 | 7.4E-07 |
| **Allograft Rejection** | 1.91 | 7.4E-07 |
| **Complement** | 1.80 | 3.2E-05 |
| **KRAS Signalling Up** | 1.74 | 1.4E-04 |
| **IL2 STAT5 Signalling** | 1.72 | 1.4E-04 |
| **Coagulation** | 1.67 | 1.4E-03 |
| Apical Junction | 1.64 | 4.8E-04 |
| **Interferon Gamma Response** | 1.62 | 1.0E-03 |
| Angiogenesis | 1.56 | 3.8E-02 |
| **Apoptosis** | 1.54 | 5.4E-03 |
| UV Response Up | 1.45 | 3.3E-02 |
| **KRAS Signalling Down** | -1.36 | 1.6E-02 |
| **Bile Acid Metabolism** | -1.60 | 1.9E-03 |
| **Fatty Acid Metabolism** | -1.63 | 1.8E-04 |
| **Oxidative Phosphorylation** | -2.07 | 1.1E-09 |
| **Adipogenesis** | -2.19 | 1.0E-10 |
| Reactome Gene Set (1635 gene sets) | | |
| **Interleukin 10 Signalling** | 2.16 | 4.9E-06 |
| **Immunoregulatory Interactions Between a Lymphoid Non-Lymphoid Cell** | 2.02 | 4.2E-06 |

| | | |
|---|---|---|
| Elastic Fibre Formation | 2.01 | 6.7E-04 |
| Molecules Associated With Elastic Fibres | 1.98 | 1.1E-03 |
| **Extracellular Matrix Organisation** | 1.93 | 1.3E-07 |
| **Purinergic Signalling In Leishmaniasis Infection** | 1.90 | 4.3E-03 |
| ECM Proteoglycans | 1.87 | 2.0E-03 |
| **GPVI-Mediated Activation Cascade** | 1.86 | 1.0E-02 |
| **Resolution of Sister Chromatid Cohesion** | 1.83 | 5.6E-04 |
| **Dap12 Interactions** | 1.83 | 1.7E-02 |
| Other Interleukin Signalling | 1.81 | 1.7E-02 |
| Syndecan Interactions | 1.79 | 2.0E-02 |
| Glycosaminoglycan Metabolism | 1.78 | 2.0E-03 |
| **Interleukin 12 Family Signalling** | 1.78 | 2.0E-02 |
| **Signalling by Interleukins** | 1.76 | 4.2E-06 |
| Rho GTPases Activate Formins | 1.75 | 2.2E-03 |
| Potassium Channels | 1.75 | 1.7E-02 |
| **Peptide Ligand Binding Receptors** | 1.75 | 4.7E-03 |
| Regulation Of Insulin Like Growth Factor IGF Transport And Uptake By Insulin Like Growth Factor Binding Proteins IGFBPS | 1.74 | 9.8E-03 |
| Nicotinamide Salvaging | 1.74 | 5.0E-02 |
| Synthesis Of Prostaglandins Pg And Thromboxane's Tx | 1.74 | 4.9E-02 |
| Mitotic Spindle Checkpoint | 1.71 | 6.9E-03 |
| Response To Elevated Platelet Cytosolic Ca2 | 1.71 | 6.3E-03 |
| Rho GTPase Effectors | 1.70 | 5.6E-04 |
| **Neutrophil Degranulation** | 1.70 | 9.3E-06 |
| Degradation Of The Extracellular Matrix | 1.70 | 1.3E-02 |
| **GPCR Ligand Binding** | 1.67 | 9.0E-04 |
| Hemostasias | 1.67 | 6.3E-06 |
| Interleukin 4 And Interleukin 13 Signalling | 1.64 | 2.5E-02 |
| **Platelet Activation Signalling And Aggregation** | 1.64 | 4.1E-03 |

| | | |
|---|---|---|
| Cell Surface Interactions At The Vascular Wall | 1.62 | 2.3E-02 |
| **Class A 1 Rhodopsin Like Receptors** | 1.62 | 1.7E-02 |
| **Leishmania Infection** | 1.62 | 7.5E-03 |
| Cell Cycle Checkpoints | 1.58 | 6.3E-03 |
| Muscle Contraction | 1.57 | 2.5E-02 |
| Separation Of Sister chromatids | 1.57 | 2.3E-02 |
| Mitotic Metaphase And Anaphase | 1.54 | 2.3E-02 |
| Mitotic Prometaphase | 1.52 | 4.9E-02 |
| Cell Cycle Mitotic | 1.45 | 1.1E-02 |
| **Signalling By GPCR** | 1.43 | 2.3E-02 |
| Metabolism Of Amino Acids And Derivatives | -1.39 | 4.0E-02 |
| **Fatty Acid Metabolism** | -1.57 | 2.5E-02 |
| **Protein Localization** | -1.68 | 1.3E-02 |
| **Activation Of Gene Expression By SREBF SREBP** | -1.79 | 4.9E-02 |
| **Peroxisomal Protein Import** | -1.82 | 2.3E-02 |
| Nr1h2 And Nr1h3 Mediated Signalling | -1.85 | 3.0E-02 |
| Peroxisomal Lipid Metabolism | -1.89 | 2.2E-02 |
| Biotin Transport And Metabolism | -1.92 | 1.0E-02 |
| **Complex I Biogenesis** | -2.05 | 2.3E-03 |
| **The Citric Acid TCA Cycle And Respiratory Electron transport** | -2.29 | 1.1E-07 |
| **Respiratory Electron Transport** | -2.29 | 4.9E-06 |
| **ATP Synthesis By Chemiosmotic Coupling And Heat Production By Uncoupling Proteins** | -2.37 | 1.1E-07 |
| KEGG Gene Set (186 gene sets) | | |
| **Nod Like Receptor Signalling Pathway** | 1.96 | 3.1E-04 |
| **Leishmania Infection** | 1.91 | 3.8E-04 |
| **Complement And Coagulation Cascades** | 1.91 | 8.5E-04 |
| Hypertrophic Cardiomyopathy HCM | 1.90 | 3.1E-04 |
| **Cytokine-cytokine Receptor Interaction** | 1.86 | 8.1E-05 |

| | | |
|---|---|---|
| **Hematopoietic Cell Lineage** | 1.81 | 1.3E-03 |
| Dilated Cardiomyopathy | 1.74 | 7.0E-03 |
| **Systemic Lupus Erythematosus** | 1.71 | 7.0E-03 |
| **Intestinal Immune Network For IGA Production** | 1.67 | 2.6E-02 |
| Hedgehog Signalling Pathway | 1.67 | 3.9E-02 |
| Cytosolic DNA Sensing Pathway | 1.63 | 4.2E-02 |
| **Lysosome** | 1.63 | 7.6E-03 |
| Cell Cycle | 1.63 | 9.2E-03 |
| Basal Cell Carcinoma | 1.57 | 4.4E-02 |
| **Gamma-R Mediated Phagocytosis** | 1.56 | 3.1E-02 |
| **Chemokine Signalling Pathway** | 1.55 | 1.1E-02 |
| Arrhythmogenic Right Ventricular Cardiomyopathy ARVC | 1.55 | 3.9E-02 |
| **Toll Like Receptor Signalling Pathway** | 1.50 | 5.0E-02 |
| Pathways in Cancer | 1.37 | 4.4E-02 |
| Parkinson's Disease | -1.56 | 3.1E-02 |
| Lysine Degradation | -1.64 | 4.2E-02 |
| Huntington's Disease | -1.66 | 1.5E-03 |
| Pyruvate Metabolism | -1.67 | 3.9E-02 |
| **Butanoate Metabolism** | -1.72 | 4.0E-02 |
| **Peroxisome** | -1.73 | 9.1E-03 |
| **Valine Leucine And Isoleucine Degradation** | -1.82 | 1.3E-02 |
| Proximal Tubule Bicarbonate Reclamation | -1.93 | 7.0E-03 |
| **Oxidative Phosphorylation** | -1.94 | 3.4E-04 |
| Retinol Metabolism | -1.99 | 3.3E-03 |
| **The TCA Cycle** | -2.09 | 9.1E-04 |
| **Biosynthesis Of Unsaturated Fatty Acids** | -2.15 | 8.5E-04 |
| **Propanoate Metabolism** | -2.15 | 8.5E-04 |

Significantly positively and negatively enriched gene sets from GSEA with respect to the hallmark, reactome and KEGG Gene set collections. Data are shown as normalised enrichment score (NES) and

adjusted *P* value. Positively enriched annotations are enriched in patients with vs without ≥F2 liver fibrosis (all annotations with an adjusted *P* value of <0.05 are shown). **In bold** are enriched annotations that were also found to be enriched within the end-of-trial analysis . (See supplemental table 5).

**Supplementary Table 5 -** Results of non-adjusted GSEA of SAT transcriptomic between NAFLD patients with vs without ≥ F2 fibrosis at the end-of-trial.

| | NES | Adjusted *P* value |
|---|---|---|
| **Hallmark Gene Set** | | |
| Allograft Rejection | 2.16 | 2.1E-09 |
| Inflammatory Response | 2.01 | 4.2E-09 |
| IL6 Jak Stat3 Signalling | 1.81 | 6.1E-04 |
| Interferon Gamma Response | 1.78 | 9.2E-06 |
| TNFα Signalling via NFκb | 1.75 | 7.8E-05 |
| Epithelial Mesenchymal Transition | 1.72 | 1.2E-04 |
| KRAS Signalling Up | 1.71 | 1.4E-04 |
| E2F Targets | 1.67 | 1.4E-04 |
| Complement | 1.67 | 1.8E-04 |
| G2M Checkpoint | 1.67 | 1.2E-04 |
| IL2 STAT5 Signalling | 1.61 | 7.4E-04 |
| Interferon Alpha Response | 1.56 | 1.3E-02 |
| Apoptosis | 1.43 | 2.1E-02 |
| Coagulation | 1.43 | 3.7E-02 |
| P53 Pathway | 1.39 | 4.6E-02 |
| Peroxisome | -1.47 | 4.4E-02 |
| KRAS Signalling Dn | -1.48 | 2.6E-02 |
| Fatty Acid Metabolism | -1.65 | 1.6E-03 |
| Bile Acid Metabolism | -1.71 | 1.6E-03 |
| Oxidative Phosphorylation | -2.17 | 2.1E-09 |
| Adipogenesis | -2.23 | 2.1E-09 |
| **Reactome Gene Set** | | |
| Immunoregulatory Interactions Between a Lymphoid and a Non Lymphoid Cell | 2.13 | 5.8E-08 |
| Generation of Second Messenger Molecules | 2.00 | 4.3E-04 |
| Chemokine Receptors Bind Chemokines | 1.98 | 7.7E-04 |

| | | |
|---|---|---|
| PD 1 Signalling | 1.95 | 7.4E-04 |
| TNFs Bind Their Physiological Receptors | 1.94 | 8.7E-04 |
| Peptide Ligand Binding Receptors | 1.93 | 8.2E-05 |
| Dap12 Interactions | 1.92 | 1.6E-03 |
| Cell Surface Interactions At The Vascular Wall | 1.87 | 3.1E-04 |
| GPVI Mediated Activation Cascade | 1.86 | 5.0E-03 |
| Antigen Activates B Cell Receptor BCR Leading to Generation of Second Messengers | 1.86 | 5.0E-03 |
| Interleukin 10 Signalling | 1.85 | 5.0E-03 |
| Purinergic Signalling In Leishmaniasis Infection | 1.85 | 7.3E-03 |
| Complement Cascade | 1.79 | 1.2E-02 |
| Interferon Gamma Signalling | 1.76 | 5.0E-03 |
| MHC Class II Antigen Presentation | 1.76 | 2.0E-03 |
| FCGR Activation | 1.75 | 1.9E-02 |
| Co-stimulation by The CD28 Family | 1.75 | 7.3E-03 |
| Class A 1 Rhodopsin Like Receptors | 1.72 | 6.1E-04 |
| GPCR Ligand Binding | 1.66 | 4.3E-04 |
| Nucleotide Binding Domain Leucine Rich Repeat Containing Receptor NLR Signalling Pathways | 1.65 | 4.4E-02 |
| Haemostasis | 1.62 | 1.9E-05 |
| TCR Signalling | 1.60 | 2.9E-02 |
| G Alpha I Signalling Events | 1.59 | 3.9E-03 |
| Resolution of Sister Chromatid Cohesion | 1.58 | 4.5E-02 |
| Neutrophil Degranulation | 1.55 | 5.9E-04 |
| Signalling by Interleukins | 1.54 | 1.5E-03 |
| Leishmania Infection | 1.53 | 1.4E-02 |
| Interferon Signalling | 1.47 | 4.7E-02 |
| Signalling by GPCR | 1.47 | 2.2E-03 |
| Platelet Activation Signalling and Aggregation | 1.46 | 2.8E-02 |
| Extracellular Matrix Organization | 1.43 | 3.6E-02 |

| | | |
|---|---|---|
| Protein Localization | -1.84 | 8.7E-04 |
| Mitochondrial Protein Import | -1.86 | 1.9E-02 |
| Pyruvate Metabolism | -1.88 | 4.5E-02 |
| Nuclear Receptor Transcription Pathway | -1.88 | 1.3E-02 |
| Citric Acid Cycle TCA Cycle | -1.94 | 1.3E-02 |
| Complex I Biogenesis | -1.96 | 3.7E-03 |
| Regulation of Cholesterol Biosynthesis by SREBP SREBF | -1.99 | 4.3E-03 |
| Activation of Gene Expression by SREBF SREBP | -2.03 | 5.0E-03 |
| Peroxisomal Protein Import | -2.04 | 1.6E-03 |
| Respiratory Electron Transport | -2.09 | 4.3E-04 |
| Respiratory Electron Transport ATP Synthesis by Chemiosmotic Coupling And Heat Production by Uncoupling Proteins | -2.12 | 1.1E-04 |
| Pyruvate Metabolism and Citric Acid TCA Cycle | -2.14 | 7.2E-04 |
| The Citric Acid TCA Cycle and Respiratory Electron Transport | -2.25 | 5.8E-08 |
| **KEGG Gene Set** | | |
| Leishmania Infection | 2.11 | 5.3E-07 |
| Cytokine-Cytokine Receptor Interaction | 2.00 | 2.8E-07 |
| Primary Immunodeficiency | 1.99 | 2.7E-04 |
| Complement and Coagulation Cascades | 1.99 | 6.0E-05 |
| Hematopoietic Cell Lineage | 1.97 | 3.9E-05 |
| B Cell Receptor Signalling Pathway | 1.85 | 4.9E-04 |
| Allograft Rejection | 1.84 | 4.6E-03 |
| Intestinal Immune Network for IGA Production | 1.84 | 2.8E-03 |
| Asthma | 1.82 | 2.8E-03 |
| Nod Like Receptor Signalling Pathway | 1.81 | 1.4E-03 |
| Toll Like Receptor Signalling Pathway | 1.79 | 1.1E-03 |
| T-Cell Receptor Signalling Pathway | 1.77 | 1.4E-03 |
| Chemokine Signalling Pathway | 1.77 | 2.3E-04 |
| Natural Killer Cell Mediated Cytotoxicity | 1.76 | 9.7E-04 |
| Antigen Processing And Presentation | 1.75 | 3.7E-03 |

| | | |
|---|---|---|
| Systemic Lupus Erythematosus | 1.75 | 2.1E-03 |
| Autoimmune Thyroid Disease | 1.75 | 1.4E-02 |
| Leukocyte Transendothelial Migration | 1.74 | 1.4E-03 |
| Graft Versus Host Disease | 1.74 | 1.4E-02 |
| Type I Diabetes Mellitus | 1.71 | 1.4E-02 |
| Cell Adhesion Molecules Cams | 1.70 | 1.9E-03 |
| FC Gamma R Mediated Phagocytosis | 1.62 | 1.2E-02 |
| Lysosome | 1.58 | 1.7E-02 |
| Regulation of Actin Cytoskeleton | 1.45 | 3.2E-02 |
| Oxidative Phosphorylation | -1.69 | 4.4E-03 |
| Beta Alanine Metabolism | -1.71 | 4.9E-02 |
| Proximal Tubule Bicarbonate Reclamation | -1.71 | 4.6E-02 |
| Glycerolipid Metabolism | -1.72 | 1.7E-02 |
| Valine Leucine and Isoleucine Degradation | -1.75 | 1.4E-02 |
| Butanoate Metabolism | -1.80 | 2.6E-02 |
| Insulin Signalling Pathway | -1.86 | 2.7E-04 |
| Pyruvate Metabolism | -1.92 | 4.6E-03 |
| Peroxisome | -2.05 | 2.3E-04 |
| Biosynthesis of Unsaturated Fatty Acids | -2.19 | 7.2E-05 |
| Propanoate Metabolism | -2.27 | 1.7E-04 |
| Citrate Cycle TCA Cycle | -2.29 | 3.6E-05 |

**Supplementary Table 6** – Targeted assessment of the expression of genes encoding 12 collagen isoforms identified all but five were significantly increased in patients with ≥F2 liver fibrosis.

| Gene | <F2 fibrosis (n=38) | | ≥F2 fibrosis (n=24) | | LogFC | *P* value | FDR |
|---|---|---|---|---|---|---|---|
| | **Log2cpm** | **Z-score** | **Log2cpm** | **Z-score** | | | |
| *COL1A1* | 9.4 ± 0.6 | -0.2 ± 1.0 | 9.7 ± 0.5 | 0.3 ± 0.8 | 0.2 | 0.12 | 0.40 |
| *COL1A2* | 10.2 ± 0.4 | -0.3 ± 1.0 | 10.5 ± 0.4 | 0.5 ± 0.9 | 0.3 | 0.007 | 0.12 |
| *COL3A1* | 11.1 ± 0.4 | -0.2 ± 1.0 | 11.4 ± 0.4 | 0.3 ± 0.9 | 0.2 | 0.09 | 0.35 |
| *COL5A1* | 7.8 ± 0.4 | -0.3 ± 1.0 | 8.1 ± 0.3 | 0.5 ± 0.9 | 0.3 | 0.003 | 0.09 |
| *COL5A2* | 8.3 ± 0.3 | -0.3 ± 1.0 | 8.6 ± 0.3 | 0.5 ± 0.9 | 0.2 | 0.008 | 0.12 |
| *COL5A3* | 8.3 ± 0.3 | 0.03 ± 1.1 | 8.2 ± 0.2 | -0.05 ± 0.9 | -0.1 | 0.36 | 0.66 |
| *COL6A1* | 10.7 ± 0.3 | -0.4 ± 0.9 | 11.1 ± 0.3 | 0.6 ± 0.8 | 0.3 | <0.0001 | 0.01 |
| *COL6A2* | 10.7 ± 0.3 | -0.4 ± 0.9 | 11.1 ± 0.3 | 0.6 ± 0.8 | 0.3 | <0.0001 | 0.01 |
| *COL6A3* | 9.6 ± 0.4 | -0.3 ± 0.9 | 9.8 ± 0.4 | 0.4 ± 1.0 | 0.2 | 0.01 | 0.16 |
| *COL12A1* | 8.7 ± 0.4 | -0.2 ± 0.9 | 8.9 ± 0.4 | 0.3 ± 1.0 | 0.2 | 0.06 | 0.31 |
| *COL14A1* | 5.9 ± 0.5 | -0.3 ± 0.9 | 6.3 ± 0.6 | 0.4 ± 1.2 | 0.4 | 0.003 | 0.09 |
| *COL24A1* | 1.3 ± 0.8 | -0.2 ± 1.0 | 1.7 ± 0.7 | 0.3 ± 0.9 | 0.3 | 0.19 | 0.50 |

Expression of each of the 12 collagen gene isoforms that were used to generate the CCGE values for patients. Expression data are shown as log2cpm and Z-scores (Z-scores were used to generate CCGE values). Log2 fold-change reflects change in log2cpm values after comparing patients without to those with ≥F2 liver fibrosis. *P* values and FDR values were extracted from DGE analysis comparing patients without to those with ≥F2 liver fibrosis. n=38 Vs. n=24 for patients without Vs. with ≥F2 liver fibrosis respectively.

**Supplementary Table 7** - Univariable associations between SAT composite collagen gene expression values and baseline anthropometric and biochemical variables

| Variables | Correlation coefficient(s) | *P* value |
|---|---|---|
| Age (years) | -0.13 | 0.32 |
| Systolic blood pressure (mmHg) | -0.09 | 0.51 |
| Diastolic blood pressure (mmHg) | -0.18 | 0.17 |
| BMI (kg/m$^2$) | 0.21 | 0.11 |
| DEXA lean body mass (kg) | -0.01 | 0.94 |
| DEXA total body fat (%) | 0.10 | 0.46 |
| MRI SAT (%) † | 0.13 | 0.30 |
| MRI VAT (%) † | -0.05 | 0.72 |
| Fasting glucose (mmol/l) † | 0.13 | 0.32 |
| Haemoglobin A1c (mmol/mol) † | 0.18 | 0.17 |
| Fasting insulin (mIU/L)† | 0.50 | **<0.0001** |
| HOMA-IR † | 0.46 | **<0.001** |
| AdipoIR †[a] | 0.35 | **0.007** |
| Triglycerides (mmol/l) † | 0.32 | **0.01** |
| Total cholesterol (mmol/l) † | -0.11 | 0.39 |
| HDL cholesterol (mmol/l) | -0.26 | **0.04** |
| AST (IU/l) † | 0.27 | **0.03** |
| ALT (IU/l) † | 0.20 | 0.13 |
| MRS-measured liver fat (%) † | 0.22 | 0.08 |
| Liver VCTE (kPa) † | 0.48 | **<0.0001** |
| FIB-4 index † | 0.13 | 0.34 |
| ELF test † | 0.12 | 0.34 |
| APRI index † | 0.22 | 0.09 |
| Adiponectin (µg/ml) † | -0.36 | **0.004** |
| Leptin (ng/ml) † | 0.23 | 0.07 |
| TNFα (pg/ml) † | 0.22 | 0.08 |

| | | |
|---|---|---|
| IL-6 (pg/ml) † | 0.34 | **0.006** |
| IL-8 (pg/ml) † | 0.24 | 0.07 |
| IL-10 (pg/ml) † | 0.30 | **0.02** |
| hs-CRP (mg/l) † | 0.13 | 0.30 |
| GDF-15 (pg/ml) | 0.14 | 0.27 |

Correlations were calculated using Pearson's correlation coefficient or Spearman's correlation coefficient (†) for normally and non-normally distributed variables respectively. Sample size n=62.
[a]n=58

**Supplementary table 8 -** Factors found to be independently associated with the presence of ≥F2 fibrosis in patients with NAFLD at the end-of-trial.

| Variables | OR (95% CI) | *P value* |
|---|---|---|
| Sex (M vs. F) | 2.23 (0.41-12.05) | 0.35 |
| Age (yrs) | 1.01 (0.93 – 1.09) | 0.86 |
| T2DM (yes) | 0.62 (1.00 – 4.02) | 0.62 |
| SAT CCGE value | 2.83 (0.92-9.73) | 0.099 |
| Adiponectin µg/ml | 0.53 (0.32-0.88) | 0.01 |
| GDF-15 (pg/ml) | 1.002 (1.000-1.003) | 0.02 |

Dependent variable was liver VCTE measurements <8.2 vs. ≥8.2 kPa (0 and 1, respectively) as a proxy threshold for the identification of ≥F2 fibrosis (end-of-study data). Sample size n=62. Logistic regression exploring the effects of sex, age, GDF-15 and adiponectin concentrations, and SAT composite collagen gene expression value and T2DM status on the likelihood that patients have ≥F2 liver fibrosis. This model was statistically significant ($X^2(6) = 30.4$, $P<0.001$) and explained 55.3% (Nagelkerke $R^2$) of the variance in the outcome variable. Hosmer and Lemeshow Test $P = 0.59$.

**Supplementary table 9 -** Factors found to be independently associated with the presence of ≥F2 fibrosis in patients with NAFLD at the end-of-trial without adiponectin concentrations.

| Variables | OR (95% CI) | *P value* |
|---|---|---|
| Sex (M vs. F) | 1.00 (0.25-3.97) | 0.99 |
| Age (yrs) | 0.95 (0.89-1.02) | 0.16 |
| T2DM (yes) | 1.12 (0.25-5.09) | 0.78 |
| SAT CCGE value | 3.59 (1.07-11.99) | **0.038** |
| GDF-15 (pg/ml) | 1.002 (1.001-1.004) | **0.008** |

Dependent variable was liver VCTE measurements <8.2 vs. ≥8.2 kPa (0 and 1, respectively) as a proxy threshold for the identification of ≥F2 fibrosis (end-of-study data). Sample size n=62. Logistic regression exploring the effects of sex, age, GDF-15 concentrations, and SAT composite collagen gene expression value and T2DM status on the likelihood that patients have ≥F2 liver fibrosis. This model was statistically significant ($X^2(5) = 21.7$, $P$=0.001) and explained 42.2% (Nagelkerke $R^2$) of the variance in the outcome variable. Hosmer and Lemeshow Test $P$ = 0.53.

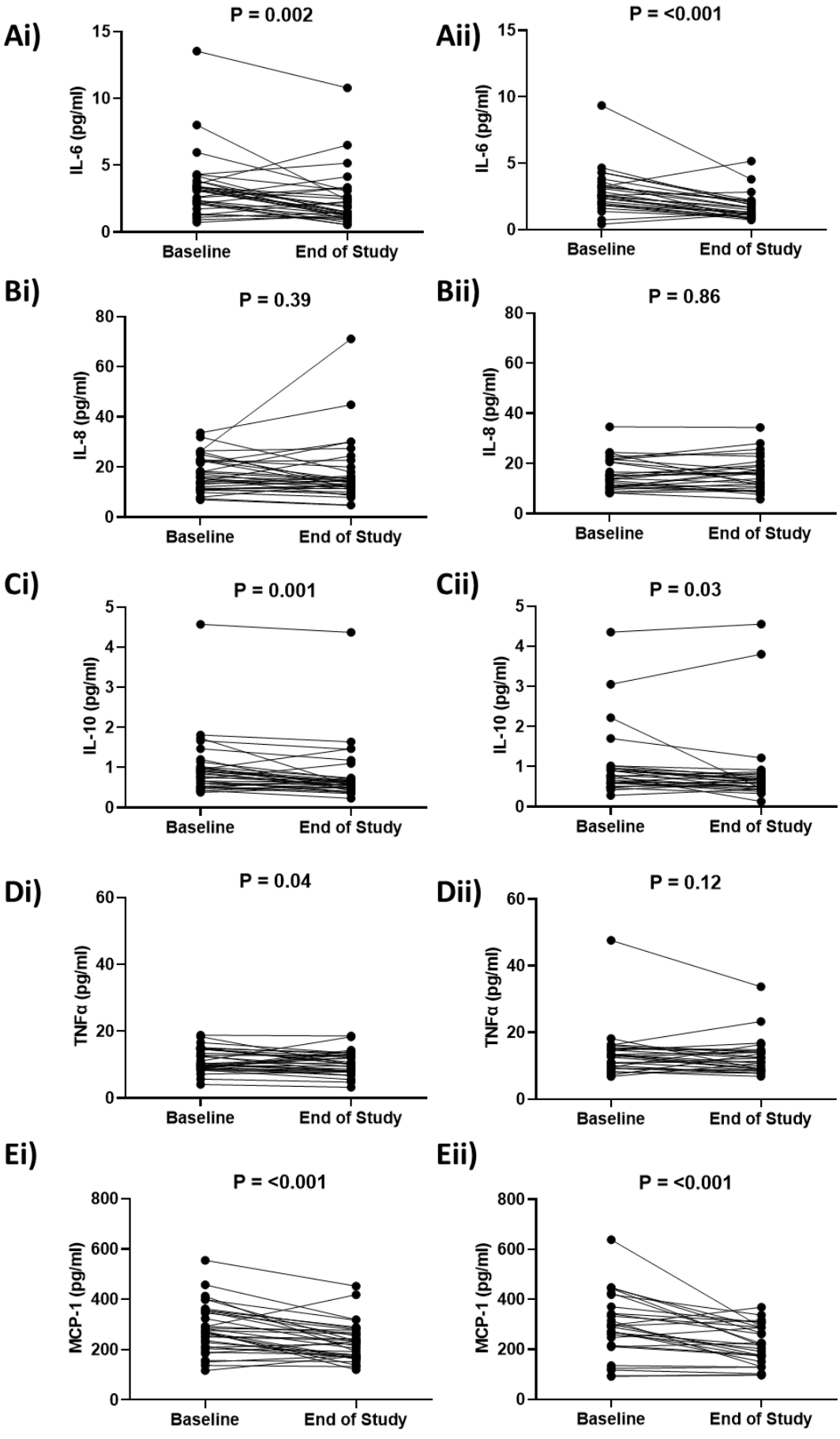
Ai)
P = 0.002
IL-6 (pg/ml)
15
10
5
0
Baseline
End of Study
Aii)
P = <0.001
IL-6 (pg/ml)
15
10
5
0
Baseline
End of Study
Bi)
P = 0.39
IL-8 (pg/ml)
80
60
40
20
0
Baseline
End of Study
Bii)
P = 0.86
IL-8 (pg/ml)
80
60
40
20
0
Baseline
End of Study
Ci)
P = 0.001
IL-10 (pg/ml)
5
4
3
2
1
0
Baseline
End of Study
Cii)
P = 0.03
IL-10 (pg/ml)
5
4
3
2
1
0
Baseline
End of Study
Di)
P = 0.04
TNFα (pg/ml)
60
40
20
0
Baseline
End of Study
Dii)
P = 0.12
TNFα (pg/ml)
60
40
20
0
Baseline
End of Study
Ei)
P = <0.001
MCP-1 (pg/ml)
800
600
400
200
0
Baseline
End of Study
Eii)
P = <0.001
MCP-1 (pg/ml)
800
600
400
200
0
Baseline
End of Study

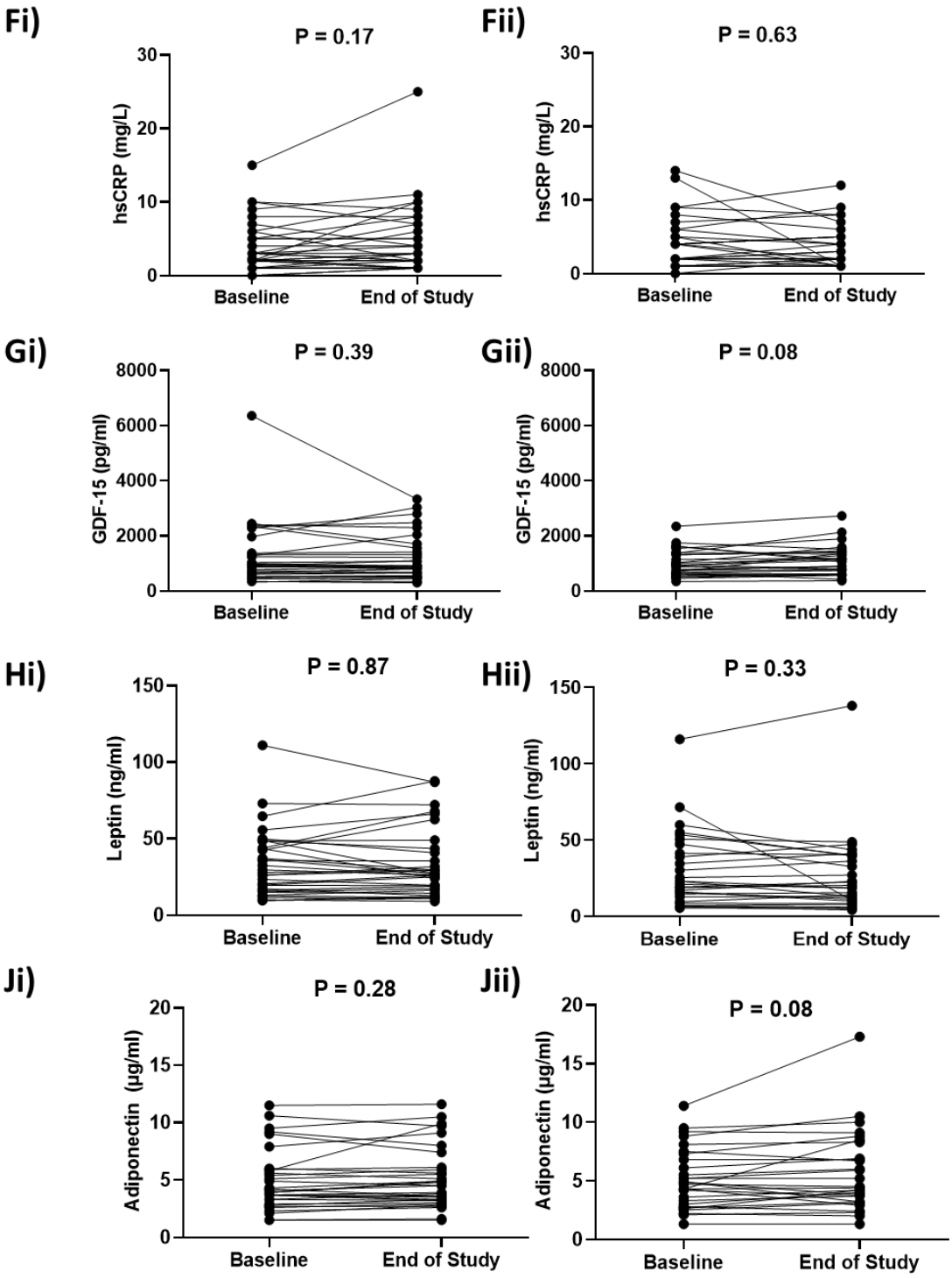


**Supplementary Figure 1 – Levels of circulating inflammatory markers and adipokines at baseline and following placebo and synbiotic treatment.** Fasted circulating IL-6, IL-8, IL-10, TNFalpha, MCP-1, hsCRP, GDF-15, Leptin and Adiponectin (A-J) for placebo (i) and synbiotic (ii) respectively. Differences between baseline and end of study measurements was tested using paired-sample Wilcoxon Signed Rank tests. Placebo group n=33, synbiotic n=29 (n=28 for Aii-Eii).

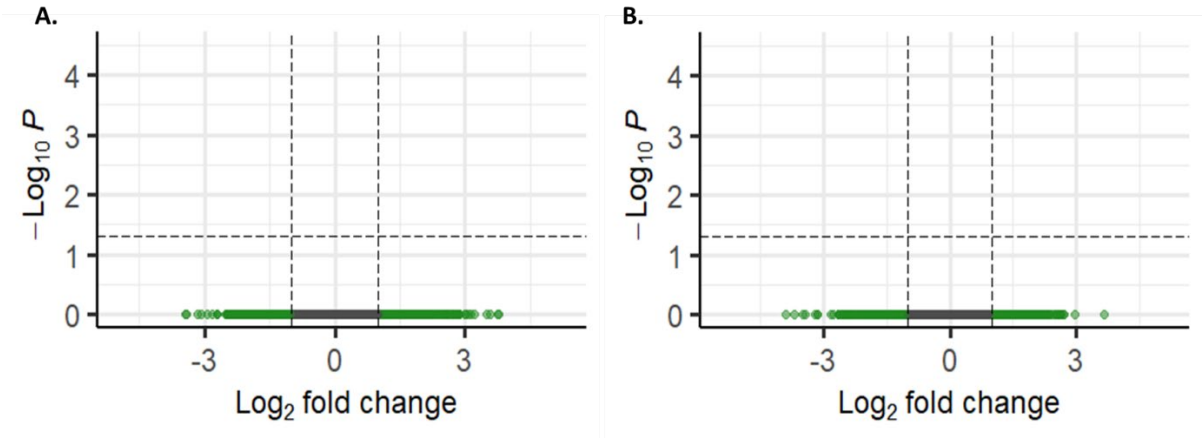


**Supplementary Figure 2 - Paired DGE analysis of baseline and end-of-study SAT protein coding genes did not identify any differentially expressed genes between the two treatment groups. A**) Analysis was carried out in n=62 patients (Synbiotic treatment n = 29 and placebo n = 33) [16]. **B**) Paired DEG analysis of baseline and end of study SAT protein coding genes between patients determined to be a synbiotic treatment responder (defined by a significant change in *Bifidobacterium* spp. over the course of the trial) [16] (n=24) vs placebo (n=33). The y-axis denotes the –Log10 *P* value obtained from DGE using edgeR's quasi-likelihood pipeline and the Benjamini-Hochberg method was used to adjust for multiple testing (FDR of <0.05 was considered to be significantly different). The x-axis denotes the Log2 fold change of SAT protein coding autosomal genes when comparing the synbiotic treatment group to the placebo group. Green dots denote genes that were not found to have a statistically significant differential expression but were found to have a $\log_2$ fold change of at least ± 1 (i.e. a 2-fold change).

A

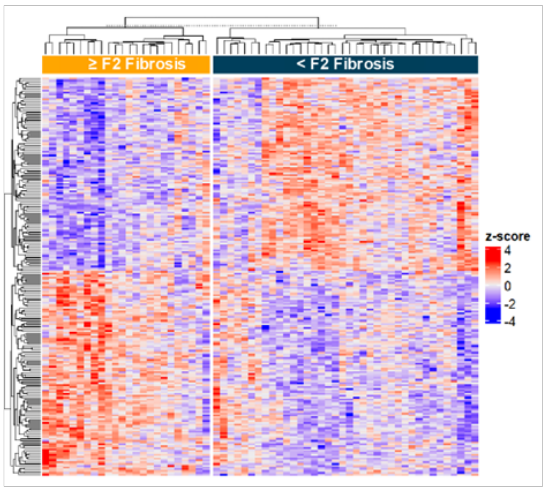
≥ F2 Fibrosis
< F2 Fibrosis
z-score
4
2
0
-2
-4

B

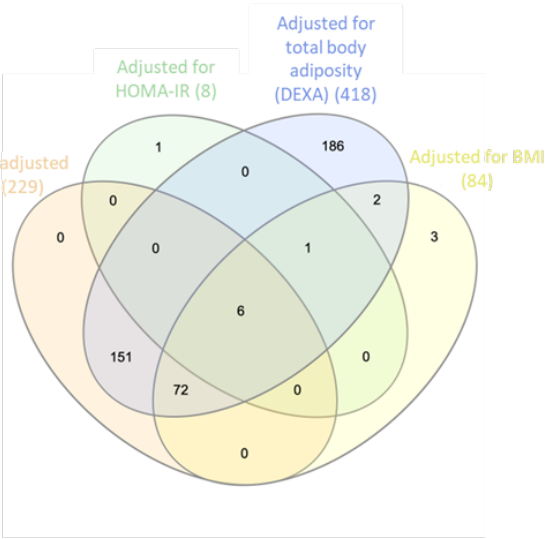
Adjusted for HOMA-IR (8)
Adjusted for total body adiposity (DEXA) (418)
Unadjusted (229)
Adjusted for BMI (84)
1
186
0
0
2
0
0
1
3
6
151
0
72
0
0

C

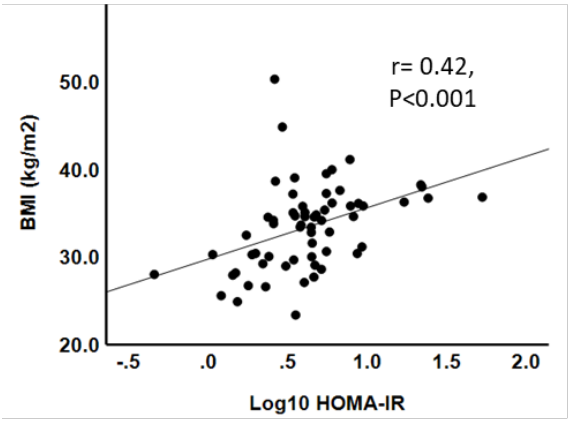
r= 0.42,
P<0.001
BMI (kg/m2)
50.0
40.0
30.0
20.0
-.5
.0
.5
1.0
1.5
2.0
Log10 HOMA-IR

D

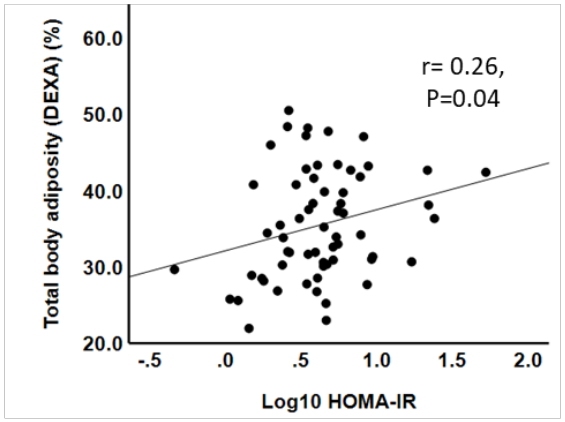
r= 0.26,
P=0.04
Total body adiposity (DEXA) (%)
60.0
50.0
40.0
30.0
20.0
-.5
.0
.5
1.0
1.5
2.0
Log10 HOMA-IR

E

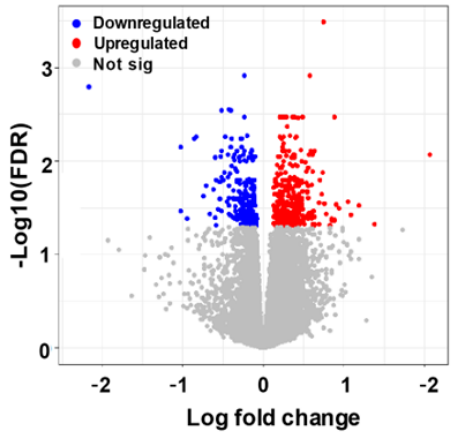
Downregulated
Upregulated
Not sig
-Log10(FDR)
3
2
1
0
-2
-1
0
1
-2
Log fold change

F

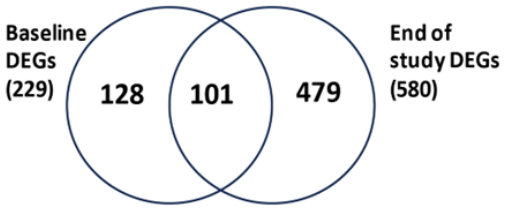
Baseline DEGs (229)
128
101
479
End of study DEGs (580)

**Supplementary Figure 3 – Differential gene expression analysis of SAT at both baseline and end of trial and the impact of adjusting for BMI on the number of DEGs at baseline. A**) Stratified and clustered heatmap of z-scores for all 229 DEGs (FDR <0.05) in SAT and associated with or without F2 liver fibrosis. Rows indicate z scores for individual genes and columns represent each SAT biopsy. When patients are stratified by liver fibrosis severity, only two distinct clusters of reciprocally regulated genes are identified. **B**) Venn diagram showing that influence of adjusting for HOMA-IR, total body adiposity and BMI on the number of DEGs between patients with vs without ≥F2 liver fibrosis. **C-D)** Scatterplots showing associations between BMI and HOMA-IR (**C**) and total body adiposity and HOMA-IR (**D**). **E**) Volcano plot of 580 DEGs (FDR <0.05) from end of study data **F**) Overlap of DEGS between baseline and end-of-trial liver fibrosis stratified DGE analysis.

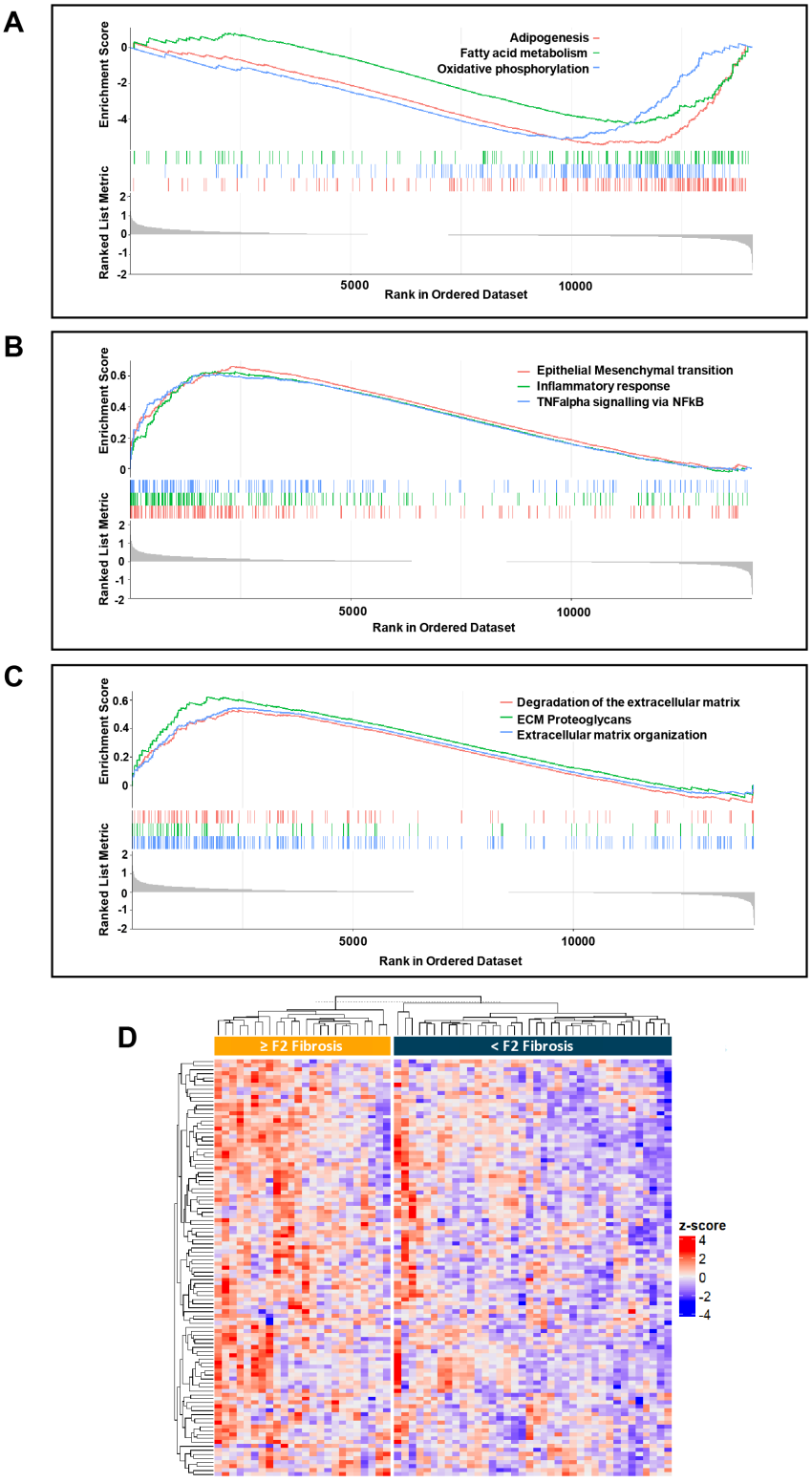


**Supplementary Figure 4 – Running normalised enrichment score plots for key pathways identified by GSEA to be enriched in SAT of patients with ≥F2 liver fibrosis. A-B)** NES plots of top negatively (**A**) and positively (**B**) enriched gene sets when comparing against the nonredundant Hallmark gene sets. **C**) NES plot of positively enriched ECM-associated gene sets when comparing against the Reactome gene sets. **D)** Stratified and clustered heatmap expression profiles of all Reactome ECM Organisation gene set following stratification of patients for liver fibrosis. Rows indicate z scores for individual genes and columns represent each SAT biopsy. When patients are stratified by liver fibrosis severity, there is a trend for higher expression of ECM genes in SAT of patients with >F2 liver fibrosis.

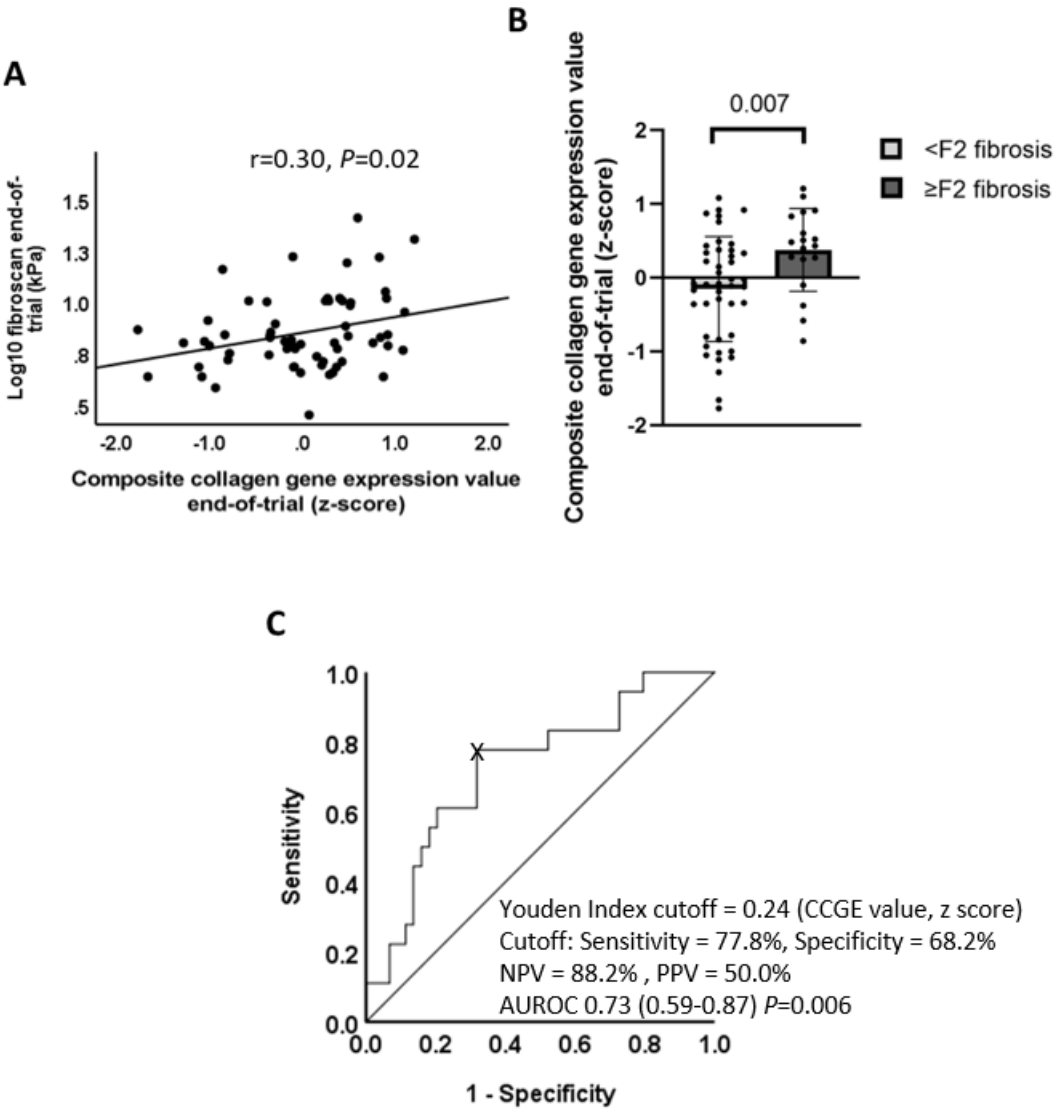


**Supplementary figure 5 – SAT CCGE at the end-of-trial was increased and had a good ability to distinguish NAFLD patients with vs without ≥F2 fibrosis (N.B. similar results were obtained in the baseline data-set analysis (see Figure 2 and 3) A**) Univariate association between CCGE values and liver-derived kPa measurements. **B**) Comparison of SAT CCGE between NAFLD patients with (n=18) vs without (n=44) ≥F2 fibrosis. **C**) ROC curve analysis of SAT CCGE and its ability to distinguish NAFLD patients with vs without ≥F2 fibrosis at the end-of-trial.

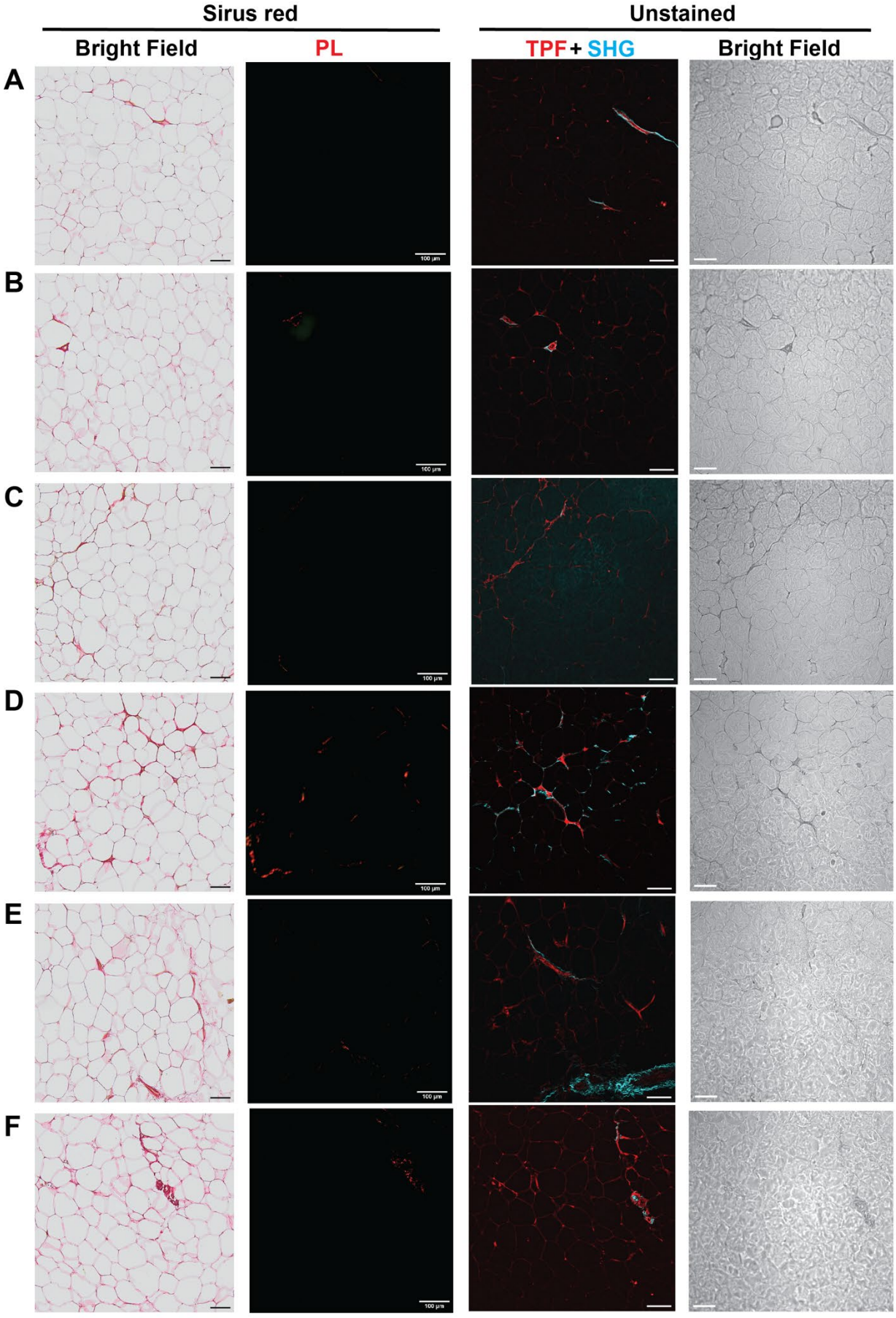
Sirus red
Unstained
Bright Field
PL
TPF + SHG
Bright Field
A
B
C
D
E
F
100 μm

**Supplementary figure 6**: **Histological imaging demonstrates presence of pericellular collagen fibres in SAT from patients with ≥F2 fibrosis and highest CCGE z scores.** Representative SAT regions of interest were selected from patients **(A -C)** with <2 liver fibrosis and the lowest and highest CCGE values (i.e. -1.15, -1.37, and -1.32 respectively) and **(D-E)** with ≥F2 liver fibrosis and the highest CCGE values (1.35, 1.01 and 1.01 respectively). Paraffin embedded serial sections (5µm) were either stained with Picrosirius red (sirus red) or left unstained. Images were acquired polarised light (PL) and bright field microscopy or with multiphoton second harmonic generation (SHG), two-photon autofluorescence (TPF) and bright-field microscopy as detailed in supplemental methods. All images were taken at 10x magnification, scale bar: 100 µm.

**Supplemental references**


1. Scorletti E, Afolabi PR, Miles EA, et al. Design and rationale of the INSYTE study: A randomised, placebo controlled study to test the efficacy of a synbiotic on liver fat, disease biomarkers and intestinal microbiota in non-alcoholic fatty liver disease. *Contemporary Clinical Trials* 2018;71:113-23.

2. Alberti KG, Eckel RH, Grundy SM, et al. Harmonizing the metabolic syndrome: a joint interim statement of the International Diabetes Federation Task Force on Epidemiology and Prevention; National Heart, Lung, and Blood Institute; American Heart Association; World Heart Federation; International Atherosclerosis Society; and International Association for the Study of Obesity. *Circulation* 2009;120(16):1640-5.

3. Fisk HL, Childs CE, Miles EA, et al. Dysregulation of Subcutaneous White Adipose Tissue Inflammatory Environment Modelling in Non-Insulin Resistant Obesity and Responses to Omega-3 Fatty Acids - A Double Blind, Randomised Clinical Trial. *Frontiers in immunology* 2022;13:922654-54.

4. Andrew S. A Quality Control Tool for High Throughput Sequence Data [Online]. *Available online at: http://www.bioinformatics.babraham.ac.uk/projects/fastqc/* 2010.

5. Ewels P, Magnusson M, Lundin S, et al. MultiQC: summarize analysis results for multiple tools and samples in a single report. *Bioinformatics* 2016;32(19):3047-48.

6. Danecek P, Bonfield JK, Liddle J, et al. Twelve years of SAMtools and BCFtools. *GigaScience* 2021;10(2).

7. Wang L, Wang S, Li W. RSeQC: quality control of RNA-seq experiments. *Bioinformatics* 2012;28(16):2184-5.

8. Frankish A, Diekhans M, Ferreira AM, et al. GENCODE reference annotation for the human and mouse genomes. *Nucleic acids research* 2019;47(D1):D766-d73.

9. Anders S, Pyl PT, Huber W. HTSeq—a Python framework to work with high-throughput sequencing data. *Bioinformatics* 2014;31(2):166-69.

10. Law CW, Zeglinski K, Dong X, et al. A guide to creating design matrices for gene expression experiments. *F1000Res* 2020;9:1444.

11. Heberle H, Meirelles GV, da Silva FR, et al. InteractiVenn: a web-based tool for the analysis of sets through Venn diagrams. *BMC Bioinformatics* 2015;16(1):169.

12. Liberzon A, Birger C, Thorvaldsdóttir H, et al. The Molecular Signatures Database (MSigDB) hallmark gene set collection. *Cell Syst* 2015;1(6):417-25.

13. Fabregat A, Jupe S, Matthews L, et al. The Reactome Pathway Knowledgebase. *Nucleic acids research* 2018;46(D1):D649-d55.

14. Kanehisa M, Goto S. KEGG: kyoto encyclopedia of genes and genomes. *Nucleic acids research* 2000;28(1):27-30.

15. Wu T, Hu E, Xu S, et al. clusterProfiler 4.0: A universal enrichment tool for interpreting omics data. *Innovation (Camb)* 2021;2(3):100141.

16. Scorletti E, Afolabi PR, Miles EA, et al. Synbiotics Alter Fecal Microbiomes, But Not Liver Fat or Fibrosis, in a Randomized Trial of Patients With Nonalcoholic Fatty Liver Disease. *Gastroenterology* 2020;158(6).